Autonomic restoration of electrical conductivity using polymer-stabilized carbon nanotube and graphene microcapsules

Susan A. Odom,[1,2] Timothy P. Tyler,[3] Mary M. Caruso,[1,2] Joshua A. Ritchey,[2] Matthew V. Schulmerich,[1,4] Scott J. Robinson,[1] Rohit Bhargava,[1,4] Nancy R. Sottos,[1,5] Scott R. White,[1,6] Mark C. Hersam,[3,7,a)] and Jeffrey S. Moore[1,2,a)]

[1]*Beckman Institute for Advanced Science and Technology, University of Illinois at Urbana-Champaign, Urbana, Illinois 61801, USA*
[2]*Department of Chemistry, University of Illinois at Urbana-Champaign, Urbana, Illinois 61801, USA*
[3]*Department of Materials Science and Engineering, Northwestern University, Evanston, Illinois 60208, USA*
[4]*Micro and Nanotechnology Laboratory, Department of Bioengineering, University of Illinois at Urbana-Champaign, Urbana, Illinois 61801, USA*
[5]*Department of Materials Science and Engineering, University of Illinois at Urbana-Champaign, Urbana, Illinois 61801, USA*
[6]*Department of Aerospace Engineering, University of Illinois at Urbana-Champaign, Urbana, Illinois 61801, USA*
[7]*Department of Chemistry and Department of Medicine, Northwestern University, Evanston, Illinois 60208, USA*

We report the use of microcapsules containing suspensions of polymer-stabilized carbon nanotubes and/or graphene flakes for the autonomic restoration of conductivity in fractured gold lines. Multilayered samples were prepared in which microcapsules were embedded in layers of epoxy above and below a glass slide patterned with gold lines. Upon sample fracture, conductivity was lost as a crack formed in the gold line. Simultaneous release of carbon nanotubes and/or graphene suspensions from capsule cores restored conductivity in minutes. We suggest a healing mechanism in which the released carbon nanomaterials bridge gaps in the gold lines. © 2012 American Institute of Physics. [http://dx.doi.org/10.1063/1.4737935]

The lifetime of an electronic device is limited when failure occurs due to a disruption of electrical conductivity as a result of fracture or debonding, both within conductive pathways and at interconnects.[1,2] In addition to integrated circuits, mechanical degradation affects the long-term performance of lithium-ion batteries. Repeated lithiation and delithiation of battery electrodes result in particle fracture and electrical isolation, ultimately resulting in a decrease in battery capacity.[3–5] Anodes in lithium-ion batteries are commonly comprised of graphitic forms of carbon, and recently carbon nanotubes have been explored as anode materials.[6,7] Autonomically restoring conductivity through the release of conductive materials from embedded capsules can extend the lifetime of electronic materials without requiring disassembly and repair of damaged components. While significant effort has been directed towards preventing failure in circuits and conductive materials, only a few examples are reported relating to the recovery of electrical performance *after* mechanical damage.[8–16] Here, we investigated improved methods for conductivity restoration of mechanically damaged electronic materials without external intervention or reliance on back-up circuits.

Our recent efforts toward restoring conductivity have focused on delivering encapsulated conductive materials to damage sites in an autonomic fashion using core-shell microcapsules.[8–10] We initially demonstrated the encapsulation of suspensions of conductive carbon nanotubes,[8] solutions of precursors to a conductive charge transfer salt,[9] and

liquid metal alloys.[10] In our publications on carbon nanotubes and charge transfer salt precursors, we manually ruptured microcapsules, demonstrating the release of conductive materials[6] and restoration of conductivity in gold lines with cracks simulated by pre-manufactured gaps (30–100 μm).[9] More recently, we developed a testing protocol in which a gold line is fractured and conductive contents are simultaneously released from capsule cores—in this case a gallium-indium eutectic—showing immediate restoration of conductivity.[10] Herein, we demonstrate the autonomic restoration of conductivity of fractured patterned gold lines using damage-triggered release of polymer-stabilized carbon nanotube and/or graphene suspensions (Figures 1(a)–1(c)). These capsules may be more compatible than charge transfer salts and liquid metal eutectics in environments such as lithium-ion batteries where anodes are often made from graphitic materials. Additionally, they may reduce the potential for short circuiting of densely packed circuit components if electric field migration guides the carbon nanomaterials preferentially to the fracture sites within each gold line, as represented in Figure 2, as opposed to a random crystallization of a charge transfer salt or capillary-driven delivery of a liquid metal.

Our previous work in which carbon nanotubes were encapsulated as suspensions in chlorobenzene or ethyl phenylacetate resulted in robust, thermally stable microcapsules.[8] However, the commercially available nanotubes used in these suspensions did not disperse well in solvents, leading to aggregation of the nanotubes, which was visible under optical microscopy. To improve the efficient release and assembly of carbon nanomaterials upon capsule rupture in this study, we employed the conducting polymer poly(3-

---

a)Authors to whom correspondence should be addressed. Electronic addresses: m-hersam@northwestern.edu and jsmoore@illinois.edu.
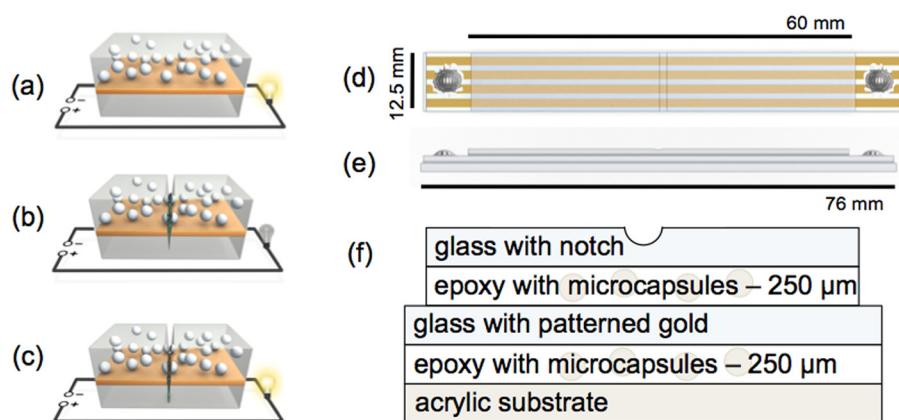
FIG. 1. Representation of conductivity restoration in a gold line (a) before damage when the sample and microcapsules are intact; (b) immediately after damage, showing fracture of gold line and release of SWCNTs and/or graphene from microcapsules; and (c) after restoration, where the conductive particles have bridged the gap in the gold line. Schematics representing test sample geometry: top view (d) and side view (e) in proportion to one another and a side view of the sample showing contents of the layers (f).

hexylthiophene-2,5-diyl) (P3HT) as an additive to achieve stable carbon nanotube and/or graphene suspensions in the non-polar solvent *o*-dichlorobenzene (DCB), guided by recent results demonstrating high single-walled carbon nanotube (SWCNT) solubilities in DCB using P3HT.[17] Additionally, SWCNT catalyst particles and carbonaceous impurities were removed via ultracentrifugation before preparing the DCB core solutions to further improve the dispersion and purity of SWCNTs.[18,19] The electrical behavior of these suspensions was analyzed by depositing the solution onto gold lines with pre-fabricated 5 μm gaps. When a 5 V potential was applied across the gap by attaching probes from a Wheatstone bridge to each end of a gold line, the nanotubes preferentially migrated to the gap in the gold line as observed via optical microscopy (Figure S2).[24] The migration is visible when a suspension is added to the gap; the color becomes increasingly darker at the gap in the gold line, while the surrounding liquid becomes transparent, showing that the carbon nanotubes have moved to the gap. This result is consistent with previous observations of electric field-driven migration of carbon nanotubes.[20–22]
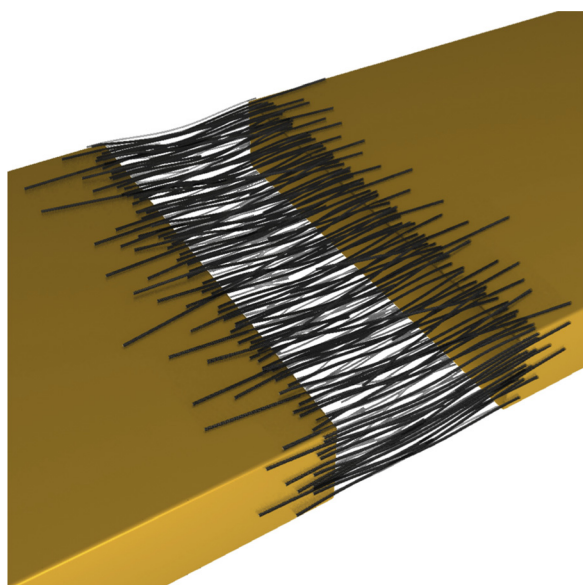
FIG. 2. An ideal representation of carbon nanotubes bridging a gap in a gold line with preferential orientation due to electric field migration. This image is not drawn to scale.

After establishing the feasibility of conductivity restoration of these carbon nanomaterial suspensions, poly(urea-formaldehyde) microcapsules were fabricated by *in situ* polymerization of urea and formaldehyde around a core of P3HT-stabilized suspensions of carbon nanomaterials in DCB. In contrast to our previous microcapsules containing carbon nanotube suspensions,[8] the current core suspensions showed no evidence of SWCNT aggregation when analyzed by optical microscopy. In addition to producing SWCNT microcapsules, we also synthesized microcapsules containing suspensions of few-layer graphene and a combination of SWCNTs and graphene. TEM images of the initial suspensions are shown in Figures 3(a)–3(c). In total, we prepared core-shell microcapsules from the following three suspensions: (i) 1:1::SWCNT:P3HT in DCB (Figures 3(d) and 3(g)); (ii) 1:1:2::SWCNT:graphene:P3HT in DCB (Figures 3(e) and 3(h)); and (iii) 1:1::graphene:P3HT in DCB (Figures 3(f) and 3(i)). In all cases, the concentration of carbon nanomaterials was 0.5 mg/ml and the P3HT was incorporated at 0.5 mg/ml. Microcapsules from all three suspensions were thermally stable (see TGA in Figure S3) and free-flowing, and showed no significant leaching over the course of the study.

Following microcapsule fabrication, initial rupture tests suggested the release of conjugated material. Optical microscopy of microcapsules compressed between glass slides showed the release of colored liquid (Figure S4). To more conclusively confirm that all components were properly suspended and released upon rupture, rather than one or more components being incorporated into the poly(urea-formaldehyde) shell wall, capsule cores were isolated for spectroscopic analysis and electron microscopy.

To isolate each type of core, a few hundred milligrams of microcapsules were crushed between two glass slides. The core liquid was then extracted and placed on a glass slide. The DCB subsequently evaporated, yielding dry films of the core components. The films were analyzed by ultraviolet-visible-near infrared (UV-vis-NIR) and Raman spectroscopy, and the results were compared to spectra obtained from dried films from the unencapsulated original core materials. Raman spectroscopy (Figure 4(b)) showed G band features around 1580 cm^{-1} associated with carbon nanotubes and graphene, where the presence of split G$^+$ and G$^-$ peaks are characteristic of SWCNTs.[23] Additionally, the second order Raman scattering peak at around 2700 cm^{-1} is characteristic
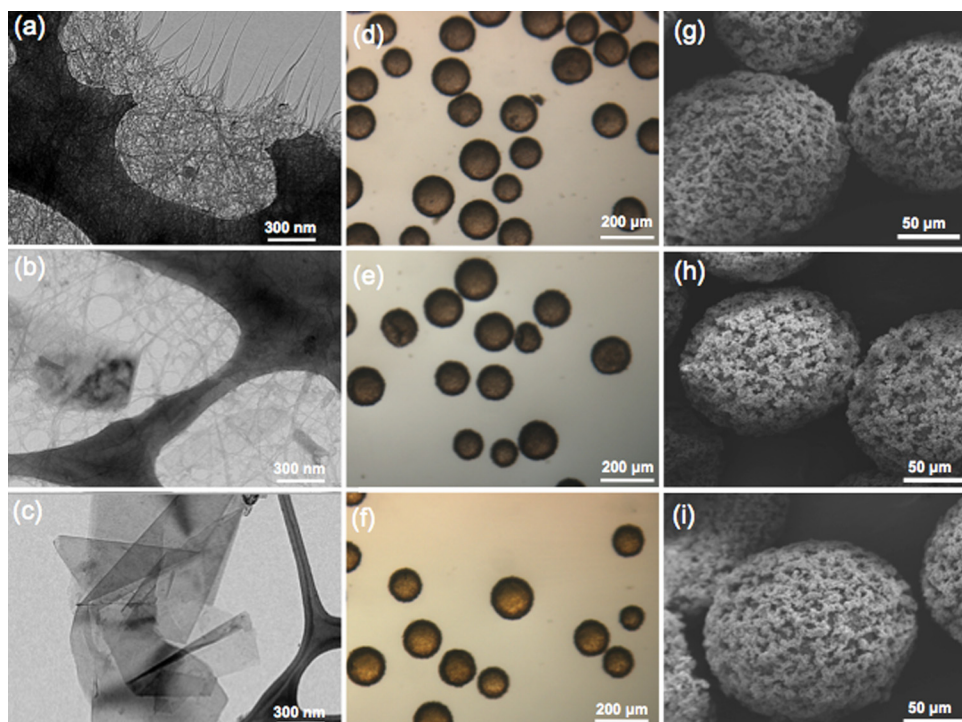
FIG. 3. TEM images of dried initial suspensions on lacy carbon grids (a)–(c), optical microscopy images of resultant microcapsules suspended in mineral oil (d)–(f), and SEM images of resultant microcapsules coated with Au/Pd (g)–(i) containing (i) 1:1::P3HT:SWCNT in DCB (a, d, g), (ii) 2:1:1::P3HT:SWCNT:graphene in DCB (b, e, h) and (iii) 1:1::P3HT:graphene in DCB (c, f, i).

of graphitic carbon and therefore is present in both SWCNT and graphene samples. These spectra were consistent with spectra of the initial suspensions before encapsulation, suggesting that both SWCNTs and graphene were released from the microcapsules upon rupture (Figure 4(a)). UV-vis-NIR spectrophotometry of films of the dried released cores (Figure 4(d)) and initial suspensions (Figure 4(c)) was also supportive of the release of carbon nanomaterials. In particular, the peak at 500–600 nm corresponds to the absorption of P3HT, while the peak centered about 1000 nm is the second-order semiconducting optical transition in arc discharge SWCNTs, often denoted as S22. The subtle peak at 700–800 nm is attributed to the first-order metallic SWCNT optical transition, M11. These SWCNT peaks are absent in
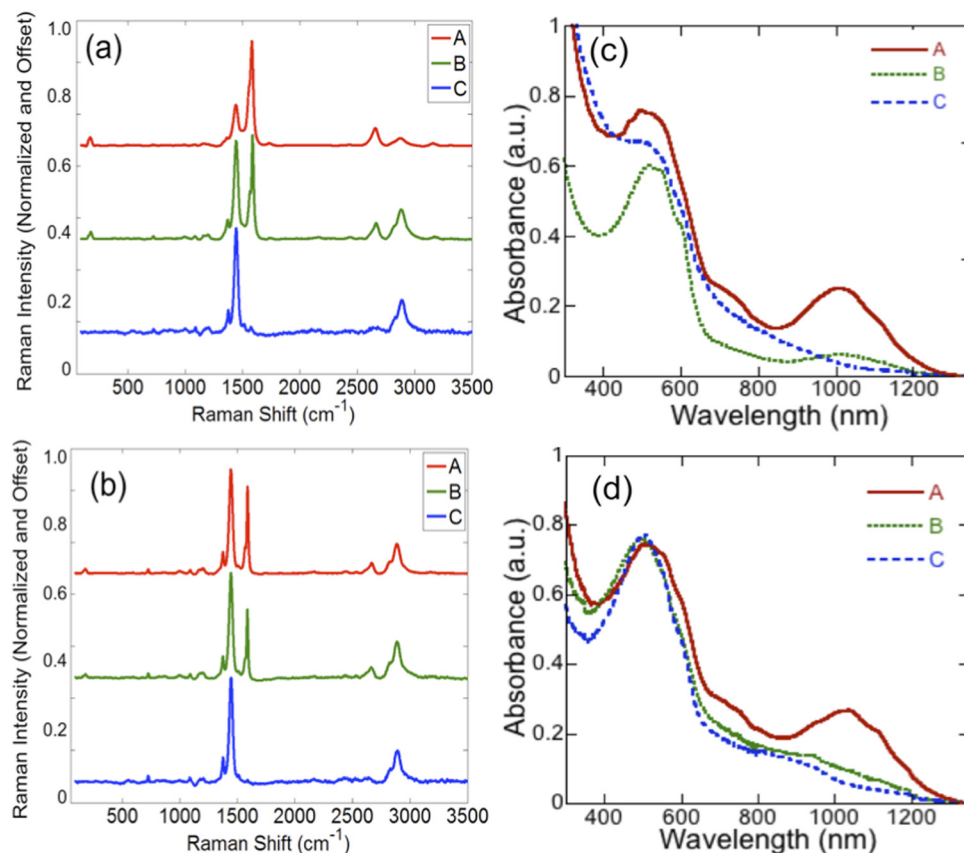
FIG. 4. Raman (a) and (b) and UV-vis-NIR (c) and (d) spectra of films of dried suspensions before incorporation into microcapsules (a) and (c) and dried suspensions after release from microcapsule cores (b) and (d), where suspensions contained 1:1::P3HT:SWCNT (A, red), 2:1:1::P3HT:SWCNT:graphene (B, green), and 1:1::graphene:P3HT (C, blue). Absorbance spectra display P3HT absorption at around 500–600 nm, the first-order metallic SWCNT optical transition at 700–800 nm, and the second-order semiconducting SWCNT optical transition around 1000 nm. Raman spectra show G band features at ca. 1580 cm^{-1} and second order G' Raman scattering peaks at ca. 2700 cm^{-1}.

the graphene-only case since they are only found in carbon nanotubes. AFM images were also acquired to analyze the components of released cores. AFM images of dried films from initial suspensions (Figure S5) and released cores (Figure S6) showed similar characteristics, although evidence of SWCNT release is more conclusive than the images of cores from graphene-containing capsules.

After confirming the release of both SWCNTs and graphene from their respective microcapsules, we tested the ability of these released suspensions to restore conductivity in fractured gold lines using the sample geometry shown in Figures 1(d)–1(f). A glass slide was patterned on one side with gold lines via e-beam deposition, which were 1.5 mm wide and spaced 1.5 mm apart. The 125–180 μm diameter microcapsules were incorporated into an epoxy slurry above and below the patterned slide at 30 wt. %, the maximum concentration of these capsules that can be incorporated into epoxy while maintaining a readily dispersible mixture. A layer of flexible acrylic was positioned at the bottom of the sample, and the top epoxy layer was capped with a glass slide containing a pre-made notch to guide sample fracture. The gold lines on the central layer faced the glass slide with notch. This sample geometry differs from our previous sample type used in 4-point bend testing for conductivity restoration.[10] In the current geometry, microcapsules are incorporated within both layers of epoxy, allowing for release of a greater volume of the active (core) component.

During testing, a load was applied to the sample using a 4-point bend set-up, and the displacement was increased at 0.001 mm/s until the sample fractured and conductivity was lost. The load was immediately removed from the sample, allowing the resultant crack to close to a minimum size. Different samples displayed a variety of healing behaviors within each microcapsule sample type. Samples in which conductivity was restored possessed different rates of healing and the times required until no change in normalized bridge voltage was observed (see Figures S7–S9). Samples also varied in the time before conductivity restoration began and the degree of conductivity restored (Figures 5(a)–5(c)). Sample types i, ii, and iii all displayed a similarly high number of samples showing full and partial conductivity restoration, demonstrating that both SWCNT and graphene suspensions are capable of efficient self-healing (Figure 5(d)). On average, full restoration of conductivity occurred in 25% of samples and partial restoration occurred in 50% of samples, leaving only 25% with no healing response. This is in contrast to control samples consisting of chlorobenzene microcapsules incorporated into the epoxy layers, for which none of the samples showed any observable level of conductivity restoration. We also observed healing for multiple gold lines in restored samples without observing particle bridging between neighboring lines; no cross-talk was observed during the healing process.

We have demonstrated a method for the autonomic restoration of conductivity in fractured gold lines that utilizes stabilized suspensions of two different types of carbon nanomaterials. Suspensions of SWCNTs, graphene, and combinations thereof provide partial or full restoration of conductivity in the majority of samples. No short circuiting was observed between gold lines placed 1.5 mm apart. This
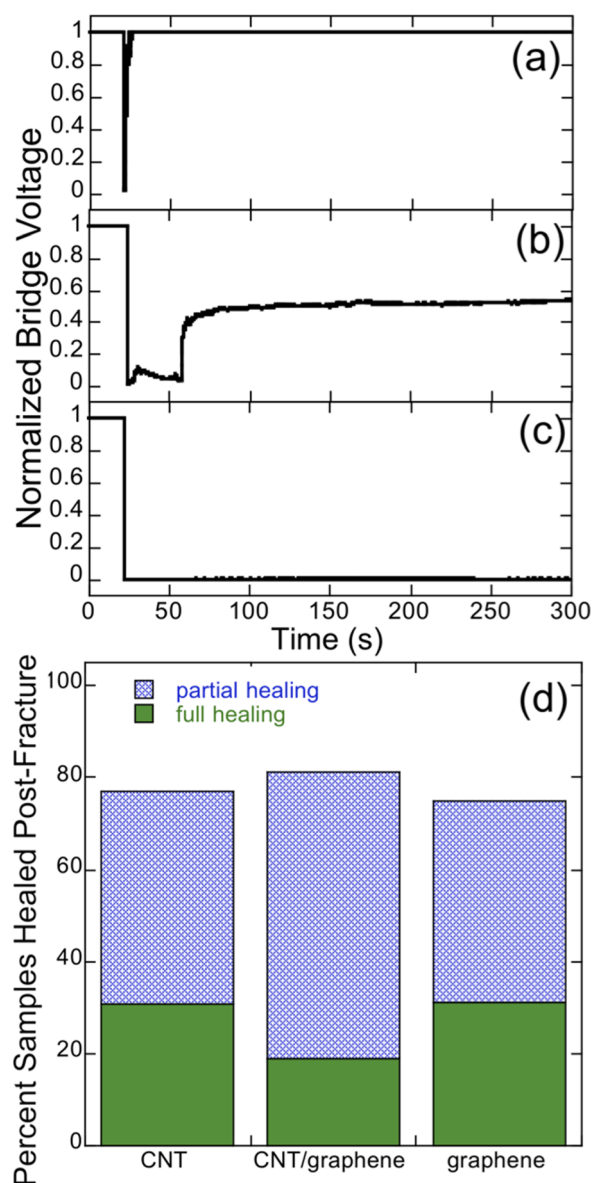
FIG. 5. (a)–(c) Normalized bridge voltage vs. time for fractured samples with microcapsules containing a 2:1:1::P3HT:SWCNT:graphene suspension. Examples are shown for full conductivity restoration (a), partial conductivity restoration (b), and no restoration (c). (d) Plot of full and partial healing percentages observed for each microcapsule type.

localized response is promising for incorporating these microcapsules in layers above integrated circuits, circumventing the need for patterning the microcapsules in specifically vulnerable regions of the circuit. These microcapsule core suspensions have the added benefit of being comprised of graphitic materials, which are commonly used in lithium-ion battery anode materials. We are interested in future studies incorporating the microcapsules into battery anodes for extending lifetimes through the distribution of released SWCNTs and/or graphene in the gaps that result from repeated lithiation/delithiation cycles as well as increasing the concentration of carbon nanomaterials in microcapsule cores.

[1]P. Viswanadham and P. Singh, *Failure Modes and Mechanisms in Electronic Packages* (Chapman & Hall, 1998).

[2]K. Jonnalagadda, Microelectron. Reliab. **42**, 253–258 (2002).

[3]J. Vetter, P. Novák, M. R. Wagner, C. Velt, K.-C. Möller, J. O. Besenhard, M. Winter, M. Wohlfahrt-Mehrens, C. Vogler, and A. Hammouche, J. Power Sources **147**, 269 (2005).

[4]H. Gabrisch, J. Wilcox, and M. M. Doeff, Electrochem. Solid-State Lett. **11**, A25 (2008).

[5]J. Christensen and J. Newman, J. Electrochem. Soc. **153**, A1019 (2006).

[6]K. Evanoff, J. Khan, A. A. Balandin, A. Magasinski, W. J. Ready, T. F. Fuller, and G. Yushin, Adv. Mater. **24**, 533 (2012).

[7]B. J. Landi, M. J. Ganter, C. D. Cress, R. A. DiLeo, and R. P. Raffaelle, Energy Environ. Sci. **2**, 638 (2009).

[8]M. M. Caruso, S. R. Schelkopf, A. C. Jackson, A. M. Landry, P. V. Braun, and J. S. Moore, J. Mater. Chem. **19**, 6093 (2009).

[9]S. A. Odom, M. M. Caruso, A. D. Finke, A. M. Prokup, J. A. Ritchey, J. H. Leonard, S. R. White, N. R. Sottos, and J. S. Moore Adv. Funct. Mater. **20**, 1721 (2010).

[10]B. J. Blaiszik, S. L. B. Kramer, M. E. Grady, D. A. McIllroy, J. S. Moore, N. R. Sottos, and S. R. White, Adv. Mater. **24**, 398 (2012).

[11]S. A. Odom, S. Chayanupatkul, B. J. Blaiszik, O. Zhao, A. C. Jackson, P. V. Braun, S. R. White, and J. S. Moore, Adv. Mater. **24**, 2578 (2012).

[12]K. A. Williams, A. J. Boydston, and C. W. Bielawski, J. R. Soc., Interface **4**, 359 (2007).

[13]S. Gupta, Q. Zhang, T. Emrick, A. C. Balazs, and T. P. Russell, Nature Mater. **5**, 229 (2006).

[14]R. Verberg, A. R. Dale, P. Kumar, A. Alexeev, and A. C. Balazs, J. R. Soc. Interface **4**, 349 (2007).

[15]G. V. Kolmakov, R. Revanur, R. Tangirala, T. Emrick, R. P. Russel, A. J. Crosby, and A. C. Balazs, ACS Nano **4**, 1115 (2010).

[16]K. Kratz, A. Narasimhan, R. Tangirala, S. Moon, R. Revanur, S. Kundu, H. S. Kim, A. J. Crosby, T. P. Russell, R. Emrick, G. Kolmakov, and A. C. Balazs, Nat. Nanotechnol. **7**, 87 (2012).

[17]H. W. Lee, W. You, S. Barman, S. Hellstrom, M. C. LeMieux, J. H. Oh, S. Liu, T. Fujiwara, W. M. Wang, B. Chen, Y. W. Jin, J. M. Kim, and Z. Bao, Small **5**, 1019 (2009).

[18]M. J. O'Connell, S. M. Bachilo, C. B. Huffman, V. C. Moore, M. S. Strano, E. H. Haroz, K. L., Rialon, P. J. Boul, W. H. Noon, C. Kittrell, J. Ma, R. H. Hauge, R. B. Weisman, and R. E. Smalley, Science **297**, 593 (2002).

[19]M. S. Arnold, A. A. Green, J. F. Hulvat, S. I. Stupp, and M. C. Hersam, Nat. Nanotechnol. **1**, 60 (2006).

[20]K. Yamamoto, S. Akita, and Y. Nakayama, Jpn. J. Appl. Phys., Part 2 **35**, L917 (1996).

[21]C. Park, J. Wilkinson, S. Banda, Z. Ounaies, K. E. Wise, G. Sauti, P. T. Lillehei, and J. S. Harrison, J. Polym. Sci., Part B: Polym. Phys. **44**, 1751 (2006).

[22]M. Ganzhorn, A. Vijayaraghavan, A. A. Green, S. Dehm, A. Voigt, M. C. Hersam, and R. Krupke, Adv. Mater. **23**, 1734 (2011).

[23]M. S. Dresselhaus, G. Dresselhaus, R. Saito, and A. Jorio, Phys. Rep. **409**, 47 (2005).

[24]See supplementary material at http://dx.doi.org/10.1063/1.4737935 for details on our microcapsule fabrication and characterization, four-point bend sample fabrication, and testing including the Wheatstone bridge setup, thermogravimetric analysis, AFM images, and additional optical microscope images and diagrams.